Chinese Chemical Letters 33 (2022) 5042–5046

Contents lists available at ScienceDirect

Chinese Chemical Letters

journal homepage: www.elsevier.com/locate/cclet

BODIPY 493 acts as a bright buffering fluorogenic probe for super-resolution imaging of lipid droplet dynamics

Jie Chen[a,b], Wenjuan Liu[a,b], Xiangning Fang[a,b], Qinglong Qiao[a], Zhaochao Xu[a,*]

[a] CAS Key Laboratory of Separation Science for Analytical Chemistry, Dalian Institute of Chemical Physics, Chinese Academy of Sciences, Dalian 116023, China
[b] University of Chinese Academy of Sciences, Beijing 100049, China

ARTICLE INFO

Article history:
Received 23 March 2022
Revised 31 March 2022
Accepted 31 March 2022
Available online 3 April 2022

Keywords:
Lipid droplet
Super-resolution imaging
Fluorescent probe
Brightness
Buffering

ABSTRACT

The need for temporal resolution and long-term stability in super-resolution fluorescence imaging has motivated research to improve the photostability of fluorescent probes. Due to the inevitable photobleaching of fluorophores, it is difficult to obtain long-term super-resolution imaging regardless of the self-healing strategy of introducing peroxide scavengers or the strategy of fluorophore structure modification to suppress TICT formation. The buffered fluorogenic probe uses the intact probes in the buffer pool to continuously replace the photobleached ones in the target, which greatly improves the photostability and enables stable dynamic super-resolution imaging for a long time. But the buffering capacity comes at the expense of reducing the number of fluorescent probes in targets, resulting in low staining fluorescence intensity. In this paper, we selected BODIPY 493, a lipid droplet probe with high fluorescence brightness, to explore the dynamic process of lipid droplet staining of this probe in cells. We found that BODIPY 493 only needs very low laser power for lipid droplet imaging due to the high molecular accumulation in lipid droplets and the high brightness, and the spatiotemporal resolution is greatly improved. More importantly, we found that BODIPY 493 also has a certain buffering capacity, which enables BODIPY 493 to be used for super-resolution imaging of lipid droplet dynamics. This work reminds researchers to coordinate the buffering capacity and brightness of fluorogenic probes.

Lipid droplets (LDs) are key organelles for lipid metabolism and energy homeostasis in cells [1], and have recently been found to have physiological functions such as relieving cellular stress and resisting bacterial invasion [2–5]. The functions of LDs are accomplished during the dynamic processes of LD generation, fusion, maturation, division, and interactions with other organelles [6–8]. The development of LD fluorescent probes has become a hot topic in recent years [9–11]. In particular, super-resolution fluorescence imaging has broken the diffraction limit, realizing the resolution of LDs and the interaction network with other organelles at the nanometer level [12,13]. However, the super-resolution imaging of the dynamic process of LDs has always been a challenge due to the poor photostability of fluorescent probes in super-resolution fluorescence imaging [14–18].

In our previous work, we developed a buffering fluorogenic probe LD-FG for LD to overcome the photobleaching and achieve stable super-resolution fluorescence imaging of LD dynamics (Fig. 1) [12]. The sensitivity of LD-FG to hydrogen bonding results in strong fluorescence emission after entering LDs and fluorescence quenching outside the LDs. The key point is that only a part of the intracellular probes entered the LDs, and the other part existed in the periphery of the LDs and acted as buffer pools. When the probes in the LDs are photobleached, the intact probes in the buffer pool will be quickly replenished into the LDs to achieve stable imaging. LD-FG has been shown to be useful for SIM imaging of various dynamic processes such as LD formation, decomposition, fusion. However, the buffering capacity comes at the expense of reducing the number of fluorescent probes in LDs, resulting in low fluorescence intensity in LDs and restricting the improvement of spatial resolution in super-resolution imaging. Therefore, in our study we are looking for a synergistic improvement of probe buffering capacity and emission brightness.

BODIPY dyes have high molar extinction coefficients and quantum yields, and are currently known dyes with the highest luminescence brightness [19,20]. Due to its lipophilicity, BODIPY dyes are often used to stain lipids, including cell membranes and LDs [21]. BODIPY 493 is the most commonly used green fluorescent LD probe with high selectivity to LDs and high brightness [22]. In this paper, we explored the buffering capabilities of BODIPY 493

* Corresponding author.
E-mail address: zcxu@dicp.ac.cn (Z. Xu).

https://doi.org/10.1016/j.cclet.2022.03.120
1001-8417/

Table 1
Optical properties of LD-FG and BODIPY 493 in various solvents.

Probe	Solvent	λ_{abs} (nm)	λ_{em} (nm)	Stokes shift (nm)	ε (L mol^{-1} cm^{-1})	φ^a	Brightness
BODIPY 493	DCM	497	508	11	84,670	0.95	80,437
	CH_3CN	492	503	11	74,505	0.96	71,525
	DMSO	495	510	15	79,205	0.89	70,492
	EtOH	495	507	12	87,010	0.91	79,179
	H_2O	453	503	50	24,420	0.07	1709
LD-FG	DCM	442	542	100	3604	0.70	2523
	CH_3CN	437	576	139	3713	0.36	1343
	DMSO	441	598	157	3418	0.24	820
	EtOH	437	598	161	3456	0.10	346
	H_2O	415	669	254	3250	0.003	10

[a] Coumarin 153 was used to obtain relative fluorescence quantum yields (φ).

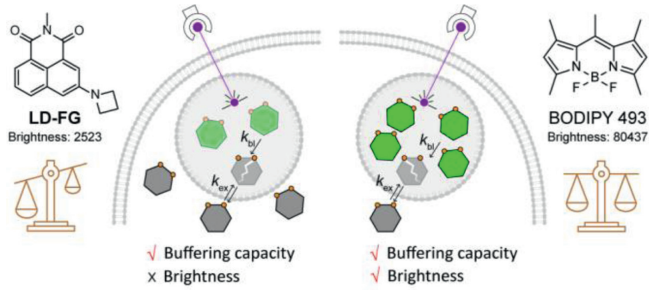

Fig. 1. LD probes LD-FG and BODIPY 493 have different buffering capacity and emission brightness, which synergistically affect the performance of buffering fluorescent probes.

(Fig. 1). Under different conditions of increasing the staining concentration, decreasing the excitation laser intensity and prolonging the imaging interval, BODIPY 493 showed good buffering imaging performance. With combination of high brightness of BODIPY 493, the spatial and temporal imaging resolution of LD dynamics can be effectively improved.

We first compared the optical properties of LD-FG and BODIPY 493 in different solvents. As shown in Table 1 and Fig. S1 (Supporting information), BODIPY 493 has much higher brightness than LD-FG in various solvents. This is mainly due to the huge difference in the molar extinction coefficients of the two probes in different solvents. LD-FG has weak light absorption capacity in all solvents ($\varepsilon = 3500$ L mol^{-1} cm^{-1}), while BODIPY 493 displays strong absorption capacity ($\varepsilon = 80{,}000$ L mol^{-1} cm^{-1}). The quantum yield (φ) of LD-FG decreases significantly when the solvent polarity increases from dichloromethane (DCM) to water. Our previous studies have demonstrated that LD-FG experienced a large change in charge density upon photoexcitation, induced more substantial vibrations of hydrogen bond could effectively quench fluorescence in protic solvents [12,23]. In contrast, BODIPY 493 exhibited high quantum yields in organic solvents ($\varphi > 0.9$). However, in water, both the absorbance and quantum yield of BODIPY 493 decreased significantly ($\varepsilon = 24{,}420$ L mol^{-1} cm^{-1}, $\varphi = 0.07$), which is likely due to the poor water solubility of BODIPY 493 and the fluorescence quenching caused by aggregation in water [24]. This significantly enhancement of fluorescence from water to organic solvents gives BODIPY 493 a good fluorogenicity for LD staining.

Improved spatiotemporal resolution depends on the brightness and stability of fluorescent probes. Probes with higher brightness can not only effectively improve the spatial resolution, but also reduce the excitation light intensity and shorten the imaging interval, thus effectively resisting photobleaching.

We first examined the effect of the high brightness of BODIPY 493 on improving temporal and spatial resolution in structure illumination microscopy (SIM) imaging. As shown in Fig. S2 (Supporting information), BODIPY 493 was able to obtain a better signal-to-noise ratio than LD-FG even when the exposure time was reduced, mainly due to the high brightness of BODIPY 493. We first chose the temporal resolution at 1.35 s/frame, the fluorescence intensity of LD-FG in LDs was about 1500, while BODIPY 493 had a ~5 fold improvement, which also made BODIPY 493 staining with high signal-to-noise ratio (~4.6 fold). For BODIPY 493, it can still maintain high brightness and signal-to-noise ratio in LDs even the temporal resolution decrease to 0.03 s/frame. These results suggest that the high brightness of BODIPY 493 allows the high temporal resolution imaging of LDs.

Exogenous fatty acids and active fatty acids produced during lipolysis and lipophagy can become toxic and ultimately trigger cell death, then the esterification of activated fatty acids will be upregulated to generate nascent LDs to avoid lipotoxicity [25]. The formation of nascent LDs is crucial for energy storage and managing cellular stress, but their size is too small to resolve [3]. BODIPY 493 has a high brightness, which improves the spatial resolution of SIM imaging, thus enabling the observation of nascent small-sized LDs.

We stimulated the biogenesis of LDs by adding oleic acid (OA) or metformin (Met) to cell culture medium, and then incubated HeLa cells with BODIPY 493 to investigate its spatial resolution in SIM imaging. As shown in Figs. 2a and b, many nascent small-sized LDs were observed in cells after OA stimulation, and the spatial resolution was significantly improved to 143 nm by comparing with the 180 nm of LD-FG in SIM imaging.

Metformin can also stimulate the generation of small LDs through the hydrolysis of LDs [26], thus the LDs diameter in Met-treated cells was visually shrunk by comparing to OA-treated cells, with the spatial resolution further coming up to 134 nm (Figs. 2c and d). These results strongly suggest that the high brightness of BODIPY 493 effectively improve the spatial and temporal resolution in super-resolution imaging, which is particularly suitable for small-sized LDs imaging.

BODIPY 493 displays strong affinity to LDs due to its high lipophilicity (Clog$P = 5.03$). This makes BODIPY 493 mainly accumulate in LDs after entering cells, which leads us to believe that BODIPY 493 had no buffering capacity at first. As the concentration of BODIPY 493-stained cells increased (from 1 to 10 μmol/L) [12], or BODIPY 493 was released into the cytoplasm as the hydrolysis of LDs (Fig. S3 in Supporting information) [27], obvious background fluorescence appeared outside LDs, which should be due to the fact that the aggregation between BODIPYs could not effectively quench the fluorescence at higher concentrations. But it also implies that BODIPY 493 exists outside LDs, providing the possibility for its buffering ability. Indeed, the large number of newly formed LDs were stained with probes in buffer pools, but caused the fluorescence quenching due to the limited buffering capability of BODIPY 493 (Fig. S4 in Supporting information).

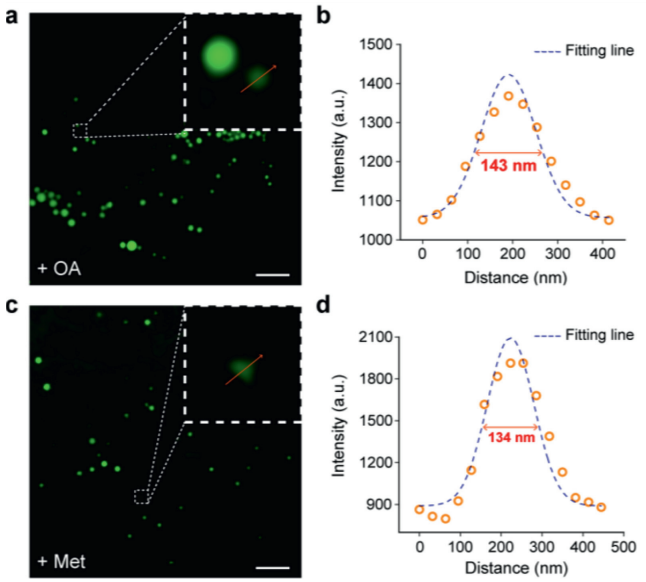

Fig. 2. Spatial resolution of BODIPY 493. (a, c) SIM images of living HeLa cells stained with 2 μmol/L BODIPY 493. (b, d) Cells were pre-treated with 200 μmol/L oleic acid for 30 min and 200 μmol/L metformin for 8 h, respectively. The plot profile of the yellow arrow in (a) and (c). Scale bar = 2 μm.

Our previous work has shown that the increasement of hydrophilicity of photobleached fluorophore allowed the exchange with intact probes in the buffer pools (Fig. 1) [12]. We defined the rate of photobleaching as k_{bl}, and the rate of exchange of bleached probe and buffer probe as k_{ex}. When $k_{ex} > k_{bl}$, the fluorescence intensity of the probe will remain stable during dynamic imaging. There are two ways to ensure that the probe exchange rate is greater than the photobleaching rate. One is to increase the buffering capacity of the probe. The higher buffering probe concentration outside LDs will increase the rate of probe exchange, as we previously reported for LD-FG. The other is to reduce the excitation laser intensity, which reduces the speed of photobleaching. This method is suitable for probes with limited buffer capacity but high brightness, such as BODIPY 493.

Next, we examined the performance of BODIPY 493 in cells to stabilize photostability by the buffering strategy. We performed FRAP (fluorescence recovery after photobleaching) experiments on living HeLa cells stained with BODIPY 493. We irradiated a selective area with a higher laser intensity (20 or 10 μW) for few seconds to cause significant photobleaching, and then changed to a mild laser intensity (4 μW) to monitor the photorecovery process under minimal photobleaching. The apparent buffering capacity of BODIPY 493 under different experimental conditions was compared by fluorescence recovery rate and final photorecovery degree.

We first compared the effect of different staining concentrations for fluorescence recovery. Increasing staining concentration can enlarge the buffer pool outside LDs, thus speeding up the exchange process. As shown in Figs. 3a and b, by incubated with 2 μmol/L BODIPY 493, the fluorescence intensity was decreased by 83% after photobleached with high power laser. Subsequently, the exchange of buffer probe made the fluorescence intensity restored to about 45% of initial fluorescence intensity (F_0) in 55 s. While the fluorescence intensity of low staining concentration could only recover from 16% to 38%. The confocal images of LDs in Fig. 3a also showed that high staining concentration resulted in clearer image after photobleaching. It is also worth mentioning that, for LD probes with high lipophilicity, excessive staining concentration would disturb the microenvironment of the LDs, and the accumulation of a large number of non-fluorogenic probes in cytoplasm would also cause high imaging background.

To further improve the apparent buffering capacity of BODIPY 493, we prolonged the imaging interval to allow more buffer probes to enter LDs for increasing the degree of fluorescence recovery. As shown in Figs. 3a and c, the fluorescence recovery rate was

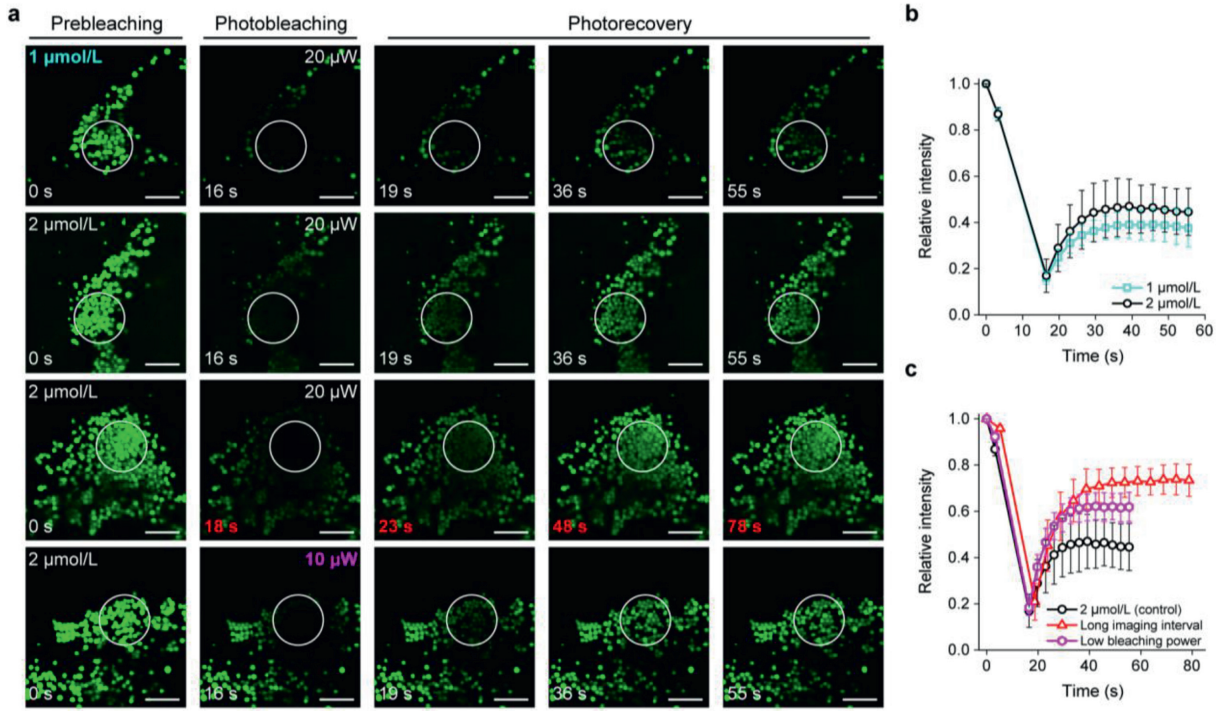

Fig. 3. (a) Confocal images of BODIPY 493 in living HeLa cells during photobleaching and photorecovery processes. White circles highlighted the bleaching area. Scale bar = 2 μm. (b, c) Relative intensity of the bleaching area during photobleaching and photorecovery processes of BODIPY 493 under different experimental conditions.

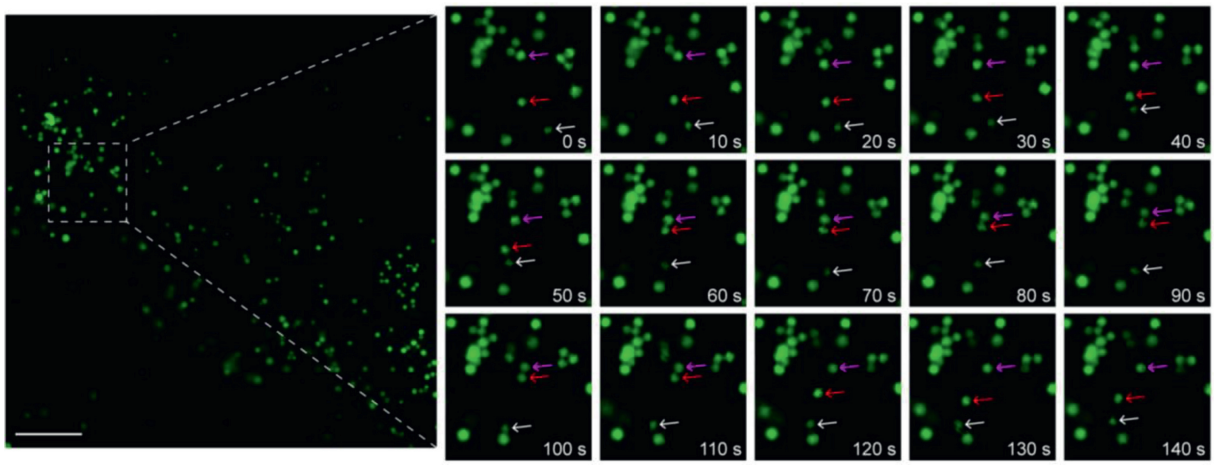

Fig. 4. Time-lapse SIM images of living HeLa cells and the enlarged images of LD movements in the boxed region. The HeLa cells were incubated with 2 μmol/L BODIPY 493 for 30 min. Scale bar = 5 μm.

significantly improved after imaging interval was extended from 3 s to 5 s with the same staining concentration. Moreover, the fluorescence intensity finally restored from 21% to 73%, and the confocal images were also brighter after fluorescence recovery (Fig. 3a). For SIM imaging, when the dynamic imaging interval was 5 s, the fluorescence intensity decreased by 48% after 25 frames; but the fluorescence intensity did not show obvious downward trend after 25 frames when imaging interval extended to 20 s (Fig. S5 in Supporting information), which was well consistent with the results of FRAP experiments. In addition, due to the excellent fluorescent properties of BODIPY 493, the laser power of imaging can be appropriately reduced to sacrifice a small amount of brightness for long-term photostable imaging. As we expected, the final fluorescence recovery degree was increased from 45% to 62% with the same staining concentration. These results indicate that increasing the staining concentration can increase the number of buffer probes to accelerate the replenishment process. Furthermore, extending imaging interval and reducing excitation laser power appropriately can also effectively minimize the impacts of photobleaching on LD dynamic imaging by BODIPY 493.

LDs are highly dynamic organelles, and the movement of LDs in cells is closely involved in lipid metabolism, energy homeostasis, signal transduction, protein degradation and interactions with other organelles [7,28]. The above results show that BODIPY 493 has high brightness and suitable buffering capacity. Therefore, BODIPY 493 was next used to track LD movement in HeLa cells by SIM imaging.

As shown in Fig. 4, the small-sized LDs were observed to move quickly in living cells. Within 0–40 s, LD1 (white arrow) gradually moved toward LD2 (red arrow), with the LD3 (magenta arrow) separated from a LDs cluster. After the contact between LD1 and LD2, the LD2 was "activated" and rapidly moved to LD3 in 10 s (50 s to 60 s), and then formed a "LD-LD complex" in the following 50 s (60 s to 110 s). Subsequently, the "LD-LD complex" disassembled and LD2 gradually returned to the activated site and moved in the direction to LD1. In addition, the reciprocating motion of small LDs was also successfully captured (Fig. S6 in Supporting information). During the tracking of LD movement, the fluorescence intensity of BODIPY 493 did not show obvious decrease (Fig. S7 in Supporting information). The above results prove that BODIPY 493 has a moderate buffering capacity, which can be used for stable super-resolution imaging of LD dynamics with time scales of tens of seconds.

In conclusion, we demonstrate that BODIPY 493 has the ability to achieve stable super-resolution imaging of LDs dynamics with a buffer strategy. BODIPY 493 benefits from its high brightness with a temporal resolution of 0.03 s/frame and a spatial resolution of 134 nm in SIM imaging, which is especially suitable for small-sized LD imaging. The apparent buffering capacity of BODIPY 493 can be effectively enhanced by increasing staining concentration, extending imaging interval and reducing excitation laser power appropriately. We believe the rationally structural modification of BODIPY dyes in future can not only retain the high brightness but also improve buffering capacity, so it would become a powerful tool for the research of LD physiology based on the high temporal and spatial resolution in super-resolution imaging.

Declaration of competing interest

The authors declare that they have no known competing financial interests or personal relationships that could have appeared to influence the work reported in this paper.

Acknowledgment

This work is supported by the National Natural Science Foundation of China (Nos. 22078314, 21878286, 21908216).

Supplementary materials

Supplementary material associated with this article can be found, in the online version, at doi:10.1016/j.cclet.2022.03.120.

References

[1] A.R. Thiam, R.V. Farese Jr, T.C. Walther, Nat. Rev. Mol. Cell Biol. 14 (2013) 775–786.
[2] M. Bosch, M. Sánchez-Álvarez, A. Fajardo, et al., Science 370 (2020) eaay8085.
[3] M.A. Welte, A.P. Gould, Biochim. Biophys. Acta, Mol. Cell Biol. Lipids 1862 (2017) 1260–1272.
[4] R. Dubey, C.E. Stivala, H.Q. Nguyen, et al., Nat. Chem. Biol. 16 (2020) 206–213.
[5] A. Romanauska, A. Köhler, Cell 174 (2018) 700–715.
[6] J.A. Olzmann, P. Carvalho, Nat. Rev. Mol. Cell Biol. 20 (2019) 137–155.
[7] S. Martin, R.G. Parton, Nat. Rev. Mol. Cell Biol. 7 (2006) 373–378.
[8] F. Wilfling, J.T. Haas, T.C. Walther, et al., Curr. Opin. Cell Biol. 29 (2014) 39–45.
[9] H. Tian, A.C. Sedgwick, H.H. Han, et al., Coord. Chem. Rev. 427 (2021) 213577.
[10] J. Zheng, S. Qin, L. Gui, et al., Chin. Chem. Lett. 32 (2021) 2385–2389.
[11] Y.H. Pan, X.X. Chen, L. Dong, et al., Chin. Chem. Lett. 32 (2021) 3895–3898.
[12] J. Chen, C. Wang, W. Liu, et al., Angew. Chem. Int. Ed. 60 (2021) 25104–25113.
[13] R. Zhou, C. Wang, X. Liang, et al., ACS Mater. Lett. 3 (2021) 516–524.
[14] Q. Qiao, W. Liu, J. Chen, et al., Angew. Chem. Int. Ed. 61 (2022) e202202961.
[15] W. Zhou, X. Fang, Q. Qiao, et al., Chin. Chem. Lett. 32 (2021) 943–946.
[16] W. Liu, Q. Qiao, J. Zheng, et al., Biosens. Bioelectron. 176 (2021) 112886.
[17] X. Wu, D. Li, J. Li, et al., Chin. Chem. Lett. 32 (2021) 1937–1941.
[18] C. Wang, W. Chi, Q. Qiao, et al., Chem. Soc. Rev. 50 (2021) 12656–12678.

[19] A. Loudet, K. Burgess, Chem. Rev. 107 (2007) 4891–4932.
[20] Y. Yan, X. Zhang, X. Zhang, et al., Chin. Chem. Lett. 31 (2020) 1091–1094.
[21] Y. Zhao, W. Shi, X. Li, et al., Chem. Commun. 58 (2022) 1495–1509.
[22] B. Qiu, M.C. Simon, Bio-protocol. 6 (2016) e1912.
[23] X. Liu, Q. Qiao, W. Tian, et al., J. Am. Chem. Soc. 138 (2016) 6960–6963.
[24] A. Romieu, C. Massif, S. Rihn, et al., New J. Chem. 37 (2013) 1016–1027.
[25] C.L. Jackson, Curr. Opin. Cell Biol. 59 (2019) 88–96.
[26] M. Espe, S. Xie, S. Chen, et al., Aquacult. Nutr. 25 (2019) 737–746.
[27] T.K. Fam, A.S. Klymchenko, M. Collot, Materials 11 (2018) 1768–1786.
[28] M.A. Welte, Biochem. Soc. Trans. 37 (2009) 991–996.